PAPER

Correlation between cyclic topology and shape memory properties of an amine-based thermoset shape memory polymer: a coarse-grained molecular dynamics study

To cite this article: Pouria Nourian et al 2022 Smart Mater. Struct. 31 105014

View the article online for updates and enhancements.

You may also like

- <u>Investigation on recovery stress and stability of hot-drawn Ni₄₇Ti₄₄Nb₅ SMA Shengshan Pan, Dong Yan, Xue Zhang et al.</u>
- Thermomechanical behavior of shape memory alloy metal matrix composite actuator manufactured by composite extrusion
- C Dahnke, A Reeb, F Pottmeyer et al.
- A newly developed Fe-based shape memory alloy suitable for smart civil engineering

engineering Kang Li, Zhizhong Dong, Yongchang Liu et al Smart Mater. Struct. 31 (2022) 105014 (11pp)

Correlation between cyclic topology and shape memory properties of an amine-based thermoset shape memory polymer: a coarse-grained molecular dynamics study

Pouria Nourian¹, Colin D Wick¹, Guoqiang Li² and Andrew J Peters^{1,*}

E-mail: apeters@latech.edu

Received 22 April 2022, revised 1 August 2022 Accepted for publication 22 August 2022 Published 6 September 2022



Abstract

Defects in crosslinked networks have a negative effect on mechanical and functional properties. In this study, an epoxy resin diglycidyl ether of bisphenol A crosslinked by a hardener 4,4-diaminodiphenyl methane with various cyclic topologies was simulated to find correlations between the mechanical/shape memory properties (i.e. glassy/rubbery elastic modulus, shape recovery ratio, and recovery stress) and cyclic topologies (i.e. number of total loops, number of defective loops (DLs), etc). The effect of cyclic topology on shape memory properties was more significant than its effect on mechanical properties, altering recovery stress by more than 25% on average. After analyzing several topological fingerprints such as total number of loops, number of DLs, and number of higher order loops, we found that the effect of cyclic topology on the mechanical/shape memory properties of the systems can be best understood by the fraction of hardeners reacted with four distinct epoxy molecules (tetra-distinctly-reacted (TDR) hardeners). By increasing the number of TDR hardeners, the network is closer to ideal, resulting in an increase in the number of higher order loops and a reduction in the number of DLs, which in turn leads to an increase in rubbery elastic modulus and shape recovery ratio to a lesser degree, but a substantial increase in recovery stress. These results suggest that utilization of experimental techniques such as semibatch monomer addition, which leads to a more expanded and defect-free network, can result in a simultaneous increase in both shape recovery ratio and recovery stress in thermoset shape memory polymers (TSMPs). Moreover, topology alteration can be used to synthesize TSMPs with improved recovery stress without significantly increasing their stiffness.

¹ College of Engineering and Science, Louisiana Tech University, Ruston, LA, 71270,

² Mechanical & Industrial Engineering Dept, Louisiana State University, Baton Rouge, LA, 70803, United States of America

^{*} Author to whom any correspondence should be addressed.

Supplementary material for this article is available online

Keywords: cyclic topology, thermoset shape memory polymer, loops, recovery stress

(Some figures may appear in colour only in the online journal)

1. Introduction

Polymer networks exhibit extraordinary mechanical properties [1, 2], and thus, have been used for the synthesis of selective membranes [3–8], elastomers and superabsorbers [9–11], and a variety of biological materials such as tissues, scaffolds, and extracellular matrices [12–21]. Shape memory polymers (SMPs), a subset of polymer networks, are stimuliresponsive materials capable of recovering from a temporary, deformed shape back to an original, memorized shape under the effect of various stimuli such as temperature, light, magnetic field, moisture, pH, or electrical current. SMPs exist as either thermoplastic or thermoset polymers depending on their crosslinked networks. Thermoset shape memory polymers (TSMPs) are a network of percolating chemical covalent bonds [22]. Their shape recovery capabilities, as well as their exceptional thermal stability and creep and chemical resistance [23], make them great candidates for use in the manufacturing of novel materials such as aerospace structures [24, 25], actuators [26-28], sealant [29], proppants [30, 31], biodegradable sutures [32], stents [33–35], and many others.

The temporary shape in SMPs can be induced through the 'hot programming' process, which consists of three stages: pre-straining at a temperature sufficiently greater than the glass transition temperature (T_g) , followed by constrained cooling of the material to a temperature below the $T_{\rm g}$, and lastly by removing the applied load and fixing a temporary shape. When heated above the $T_{\rm g}$, the material returns to its original shape. The stress the material exerts during the recovery process is known as the recovery stress. The fraction of the temporary shape recovered to the original shape is known as the recovery ratio [36]. Upon releasing the constraints at the end of the programming event, the chains are aligned with reduced entropy; upon reheating, the chains revert to their favored coil-shaped state, thus recovering the lost entropy and restoring the original shape [23, 36]. In some cases, energy can also be stored enthalpically per bond length change and bond angle change [37, 38].

Shape recovery properties (i.e. recovery stress and shape recovery ratio) are important performance-determining properties of SMPs. The current generation of TSMPs suffers from low recovery stress [38], which limits the application of these materials due to the inability of the material to support the weight of larger sample sizes [39]. Thus, finding means by which one can improve these properties in existing TSMPs has been a priority for researchers in this field. Additionally, attempts have been made to enhance the properties of SMPs through reinforcing them with carbon nanotubes [40–42], particulates [43, 44], and fibers [25, 45, 46]. While these approaches can lead to an improvement in recovery

stress, they have major drawbacks such as partial or near total loss of shape memory. Thus, more robust approaches are needed to improve both the recovery stress and shape recovery of existing TSMPs.

The effects of cyclic topology on the mechanical properties of polymer networks have been studied before, suggesting that the presence of primary loops [47–49] (which are elastically inactive [50–52]) as well as secondary loops [53–55] adversely affect the mechanical properties (i.e. elastic and storage moduli) of these networks [56–60]. TSMPs are a subclass of polymer networks, and yet, the effects of cyclic topology on their mechanical, and more importantly, shape memory properties and ultimately, the possibility of enhancing their shape memory properties through manipulation of their topological properties, have not been explored.

In this work, we aim to investigate the effects of cyclic topology on the shape memory properties of TSMPs by studying many systems that are similar to epoxy-hardener pair and crosslinking density but of different cyclic topologies. Given the large number of systems required to conduct such a study, we opt to utilize a coarse-grained (CG) model to reduce the total computational time required to carry out this study. The CG model of diglycidyl ether of bisphenol A (DGEBA) as the epoxy monomer and 4,4-diaminodiphenyl methane (DDM) as the hardener, proposed by Duan et al [61] was chosen. The advantage of this particular model over other CG models for various epoxy-hardener pairs in the literature persists in its capability to capture properties of the material at different temperatures. Almost all other CG models in the literature are only viable at a fixed temperature. Such a feature of the model is essential in calculations of shape memory properties because the shape fixity and shape recovery are temperature dependent.

The rest of the paper is organized as follows: we first introduce the details of the model and the simulations employed, followed by the results of our simulations and the statistically significant correlation among those properties and various topological properties of our systems. Finally, we discuss the physical interpretation and significance of those significant correlations. We close this work by summarizing our findings, suggesting its application in the synthesis of TSMPs, and proposing prospects for future studies.

2. Methodology

2.1. Model

The CG model used for the DGEBA-DDM pair, which is taken from [61], reduces each of the epoxy/hardener molecules into three super atoms (figure 1(a)). Harmonic forms are used

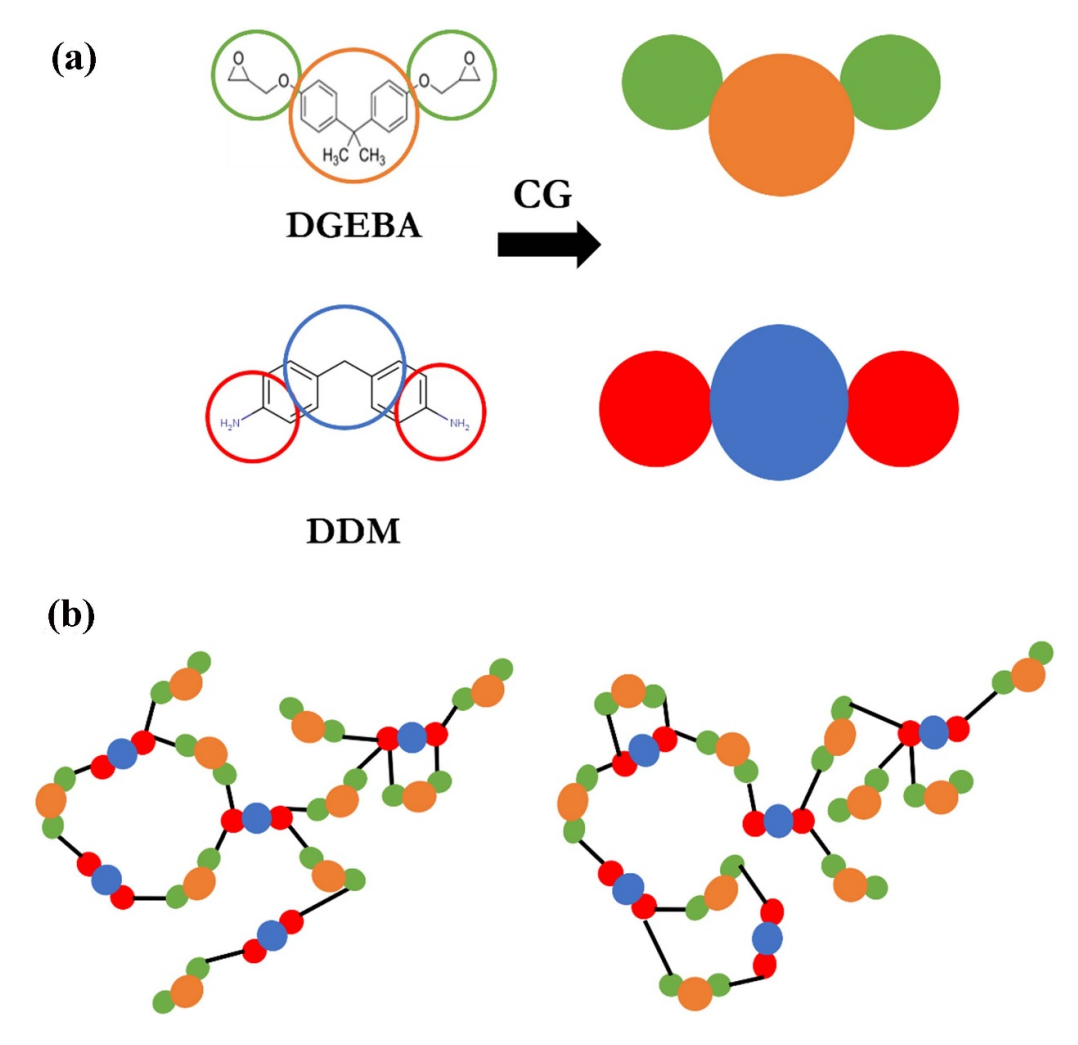


Figure 1. Plot of (a) the epoxy (DGEBA) and hardener (DDM) molecules and their representative coarse-grained model, and (b) schematic of two structures with similar crosslinking density but different cyclic topology.

for bond stretching and bending to approximate the bonded potential, and the non-bonded interactions are defined by the 12–6 Lennard–Jones (LJ) potential. The force field parameters including the mass of super atoms, bond and angle stiffness, equilibrium bond lengths and angles, and the LJ interactions parameters, i.e. the radial distance corresponding to zero inter-particle potential (σ) and potential well depth (ε) were obtained from the same work [61]. The efficacy of this model in reproducing the results of the more-accurate all-atom models (especially density and elastic modulus) was demonstrated in the original work. More complex CG forcefields can be created [62], or even the more accurate Brenner potential [63] can be used, but for the purpose of studying the effect of topology, a relatively simple form is appropriate.

2.2. Simulation details

All the simulations were conducted using the LAMMPS software package [64], in the absence of solvent, in either the constant number of atoms, pressure, and temperature (NPT) or the constant number of atoms, volume, and temperature (NVT) ensemble. A timestep of 5 fs was used in the simulations,

unless specified otherwise. Nose–Hoover thermostats and barostat [65, 66] were utilized with damping constants for temperature and pressure control equating 100 times and 1000 times the timestep, respectively. In all the simulations, the periodic boundary conditions were imposed on the cubic simulation boxes in all three directions.

2.3. Crosslinking procedure

Initial simulation boxes were prepared by using the Polymatic software [67] to randomly place 300 hardener molecules and 600 epoxy molecules in a cubic simulation box. The simulations were initialized at a temperature of 600 K. After energy minimization, the initial equilibration was performed for a duration of 500 000 steps in the NPT ensemble at a temperature of 600 K and pressure of 1 atm, with a timestep of 1 fs. The polymer rearrangement in the rubbery state occurs over timescales in orders of seconds, while the timescales accessible to MD simulations are on the order of nanoseconds. Therefore, to avoid having to run extremely long equilibrium simulations, the initialization step of the simulations is conducted at temperatures much higher than the glass transition temperature

to speed up the relaxation process. At the end of the relaxation procedure, the simulation box side length reached $\sim 78 \text{ Å}$

To create the systems with a fixed topology and a target crosslinking density (i.e. the ratio of the number of bonds between epoxy and hardener molecules to the total number of possible bonds between them) of 70%, the crosslinking procedure was conducted in NVT ensemble using 'fix bond/create' option in LAMMPS, with a timestep of 1 fs, a bond formation minimum distance (i.e. the distance indicating how close a pair of epoxy-hardener sites need to be in order to form a bond) of 7 Å for a total duration of 500000 steps, and an attempt to create bonds executed every 1000 steps. The reaction procedure was stopped once the system achieved a crosslinking density of 70%. About 25 systems with the same topology were produced and equilibrated. These 25 systems were made by equilibrating one system with 25 different initial velocities.

To create the systems with random topologies, the same procedure was conducted but with a bond formation minimum distance of 50 Å to create a system with almost 100% crosslinking density. Afterward, this system was used to generate 100 systems with different topologies by removing several epoxy-hardener bonds from the initial system to reduce the overall crosslinking density to 70%. By repeating this process 100 times, these 100 systems with different topologies were created. All these simulations were conducted with a timestep of 1 fs. Given the large bond formation minimum distance used in this approach, the systems contained long bonds. These rather long bonds were equilibrated in a stepwise manner: Initially, the bond stiffness and equilibrium distances were set to a low $(0.5 \text{ kcal mol}^{-1} \text{ Å}^{-3})$ and a high (20 Å) value, respectively. At each stage, the bond stiffness was increased, the bond equilibrium distance was reduced, and the systems were equilibrated for a duration of 50 000 steps. The procedure was conducted for a total of 15 stages.

2.4. Cooling

After the crosslinking procedure and bond relaxation were completed, the reacted systems were energy minimized and equilibrated for an additional 500000 steps in the NPT ensemble at a temperature of 600 K and pressure of 1 atm. Then, the systems were cooled down with an effective cooling rate of 20 K/1 ns to a temperature of 300 K in a stepwise manner: In each step, the temperature was reduced by 10 K, and the system was equilibrated in NPT ensemble at the current temperature and a pressure of 1 atm, for a duration of 500 000 steps. At the end of each step, a data file was saved as a starting point for the system at that temperature. It should be mentioned that this cooling rate is not experimentally achievable, but such a rate is common in MD simulations since the simulations can only capture a few nanoseconds of the system evolution [37, 68]. This rate probably overestimates the absolute shape memory properties [37], but allows for comparison between the effects of topologies which is the main focus of this work.

2.5. Elastic modulus

To determine the elastic modulus, the temperatures 300 K and 440 K (\sim 40 K above or below the system $T_{\rm g}$ [61]), were selected for calculating the glassy and rubbery elastic modulus, respectively. At each temperature, the system was first energy minimized. A linear deformation totaling 3% was imposed over ten different steps of 0.3% each. Each step included a linear deformation of $\pm 0.3\%$ was imposed over a very short period (100 steps), followed by an equilibration period of 200 000 steps. The stress in the system was obtained during the second half of the equilibration process and averaged over that period. Six total simulations were conducted for both stretching (positive deformation) and compression (negative deformation) and in all three orthogonal directions independently. Both the glassy elastic modulus (E_g) and rubbery elastic modulus (E_r) were then calculated as the slope of the stress vs. strain curve at the corresponding temperatures.

3. Programming

To determine the recovery stress and recovery ratio, the systems were first energy minimized at 440 K and then, similar to the procedure used for the calculation of elastic modulus, a linear deformation of -0.05% (compression) was imposed on them for a very short duration (ten steps) and the systems were held at fixed deformation for 9990 steps. This procedure was repeated 99 more times to reach an overall 50% compression, followed by a relaxation period with fixed deformation for a duration of 1000000 steps. The programming stress (σ_p) was calculated as the average of the stress in the system during the second half of this relaxation stage. Afterward, the systems were cooled to a temperature of 300 K with fixed deformation over a period of 1000000 steps, followed by a relaxation period at the same temperature for a duration of 1000 000 steps, during which the systems were allowed to fully relax, and experienced a small elastic spring-back by load removal. Afterward, the systems were heated up back to a temperature of 440 K with fixed deformation over a duration of 1000000 steps, followed by a relaxation period at the same temperature and with a fixed deformation. During this stage, the stress data was collected, and the recovery stress (σ_r) was calculated as the average of stress data over the second half of this period. At the final stage (i.e. the shape recovery stage), the system temperature was raised to 550 K, the stress was removed, and the system was allowed to recover from its temporary shape for a duration of 54 000 000 steps. The recovery ratio (R_r) was calculated as $R_{\rm r}(t) = \frac{\epsilon_0 - \epsilon(t)}{\epsilon_0}$, with ϵ_0 being the initial strain at the beginning of the shape recovery stage and $\epsilon(t)$ being the strain as a function of time during the recovery stage. The final recovery ratio (R_r) is calculated as the time-averaged $R_r(t)$ over the last 2000 000 steps of the shape recovery stage. The temperature at this stage was raised beyond the starting programming temperature (i.e. 550 K instead of 440 K) to essentially observed a more substantial shape recovery process. At 440 K, the systems experienced very small shape recovery $(R_{\rm r} < 0.1)$ due to the small timescales used in the simulations.

Table 1. Mean (μ) , standard deviation (σ) , and standard error (SE) of glassy elastic modulus (E_g) , rubbery elastic modulus (E_r) , shape recovery ratio (R_s) and recovery stress (σ_r) for systems with random topologies and those with a fixed topology. Results with statistical significance are highlighted in red.

Property	μ (fixed)	σ (fixed)	SE (fixed)	μ (random)	σ (random)	SE (random)	p
$E_{\rm g}$ (GPa)	3.123	0.196	0.039	3.109	0.207	0.020	0.757
$E_{\rm r}$ (GPa)	1.300	0.131	0.026	1.430	0.150	0.015066	0.0001
$R_{\rm r}$	0.681	0.089	0.017	0.631	0.067	0.006723	0.014
$\sigma_{\rm p}$ (MPa)	132.2723	14.07687	2.815373	176.8977	20.22058	2.022058	0
$\sigma_{\rm r}$ (MPa)	27.800	2.852	0.570	35.131	4.335	0.433	0

The programming procedure was applied in all 3 orthogonal directions independently, and the results were averaged.

4. Results and discussions

The results for E_g , E_r , R_r , σ_p and σ_r for both sets of systems (those with random topologies and those with a fixed topology) are plotted in figure S1, and a summary of the mean, standard deviation, and standard error for the aforementioned properties on both sets of systems are presented in table 1. Moreover, to verify whether the means of the properties of the systems with random topologies are affected by the topological properties and not just the uncertainties associated with the MD simulations, the validity of the null hypothesis with regards to the mean of the results for the two sets of systems was evaluated. The resulting p-values are presented in table 1.

As observed in table 1, the E_r , R_r , σ_p and σ_r are indeed affected by more than just the statistical uncertainties associated with the MD simulations. $E_{\rm g}$ is unaffected by the topology in a statistically significant manner because the material properties are not determined by the longer-range topological structures, but by the short-range local interactions. The difference in average $\sigma_{\rm r}$ and $\sigma_{\rm p}$ is not only statistically significant (p is less than $p < 1 \times 10^{-14}$ and $p < 1 \times 10^{-16}$, respectively) but differs by 33% and 26%, respectively, between the two populations. Furthermore, the range of the recovery stress data (i.e. the difference between the maximum and the minimum) for the systems with a fixed topology is ~ 11 MPa, compared to $\sim 24 \,\mathrm{MPa}$ for the systems with random topologies. A recent study by some of us demonstrated that the range of recovery stress data for a set of systems with various epoxyhardener pairs can be as high as ~ 40 MPa [68]. Thus, while the effect of topology on the mechanical/shape memory properties of TSMPs might not be as strong as the effect of chemical composition, manipulation of the topological properties of the system seems to be a viable method for improving mechanical/shape memory properties of these materials.

To establish a correlation between the shape memory and topological properties, we considered three 'fingerprints' of the topology involving loops. In our analysis, a loop is defined as a collection of atoms where if one starts tracing the bonds beginning at any atom in the collection, the tracing would end at that same atom. Thus, the number of loops (N) is the number of such collections in a system, the size of the loop (n) is the number of atoms in any such collection, and the mass of

the loops (m) is the sum of masses of all atoms in any such collection. Based on these definitions, the three topological fingerprints are: the number of loops (N), the average size of the loops (N_N) , defined as $N_N = \frac{\sum n_i}{N}$, and the weight-averaged size of the loops (N_W) , defined as $N_W = \frac{\sum m_i n_i}{\sum m_i}$ with m_i and n_i being the mass and the size of the ith loop, respectively. N_N and N_W can be thought of as the number and weight average molecular weight of the loops, respectively. The Pearson correlation coefficient (r) between the mechanical and shape memory properties and the aforementioned fingerprints, as well as the p-values for each correlation, is presented in table 2.

The results presented in table 2 indicate a statistically significant positive correlation between the number of loops and the programming stress, recovery stress, and shape recovery ratio. However, we do not observe any statistically significant correlations involving the rubbery elastic modulus. Yet, the effect of topology on the rubbery elastic modulus is evident from table 1. Thus, the topological fingerprints need to be further refined to capture the effect of topology on the rubbery elastic modulus.

As mentioned earlier, previous studies on the effect of cyclic topology on the mechanical properties of the polymer networks suggest that 'defective' loops (figure 2) [57] adversely affect the elastic modulus of polymer networks [47–57]. Primary DLs contain one hardener molecule that is reacted to the same epoxy molecule thus forming a single loop (figures 2(a) and (b)). These loops are described as elastically inactive and act as the endpoints of the network (figures 2(a) and (b)), which harm the network properties by inhibiting network growth and taking away epoxy molecules that could otherwise participate in network perfection. Secondary DLs (figures 2(c) and (d)) contain two hardener molecules that reacted with either one or two epoxy molecules, thus forming either a single or a double loop. While the single secondary loops can be a part of the network, the double secondary loops (figure 2(d)) do not participate in the network at all. Furthermore, their adverse effect on the storage modulus of the polymer networks has been demonstrated previously [58, 59]. Interestingly, the recovery stress and shape recovery ratio appear to have a stronger correlation with N than the rubbery elastic modulus does.

Based on this information, we opted to examine the correlation between the cyclic topology and shape memory properties of the TSMPs in the context of those studies. Given that the TSMPs are a subset of polymer networks, it is expected to see the adverse effect of the DLs on the properties of the

Table 2. Pearson correlation coefficient and its corresponding p-value among the topological fingerprints: number of loops (N), average size of the loops (N_N) and weight-averaged size of the loops (N_W) , and the mechanical and shape memory properties of the systems with random topologies: glassy elastic modulus (E_g) , rubbery elastic modulus (E_r) , shape recovery ratio (R_r) and recovery stress (σ_r) . Results with statistical significance are highlighted in red.

	N		$N_{ m N}$		$N_{ m W}$	
Property	\overline{r}	p	\overline{r}	p	\overline{r}	p
$\overline{E_{\mathrm{g}}}$	0.055	0.585	0.006	0.950	0.007	0.941
$E_{\rm r}$	0.131	0.194	0.068	0.496	0.069	0.492
$R_{\rm r}$	0.199	0.046	0.143	0.153	0.145	0.150
$\sigma_{ m p}$	0.190	0.057	0.131	0.193	0.132	0.191
$\sigma_{ m r}$	0.259	0.009	0.075	0.453	0.077	0.446

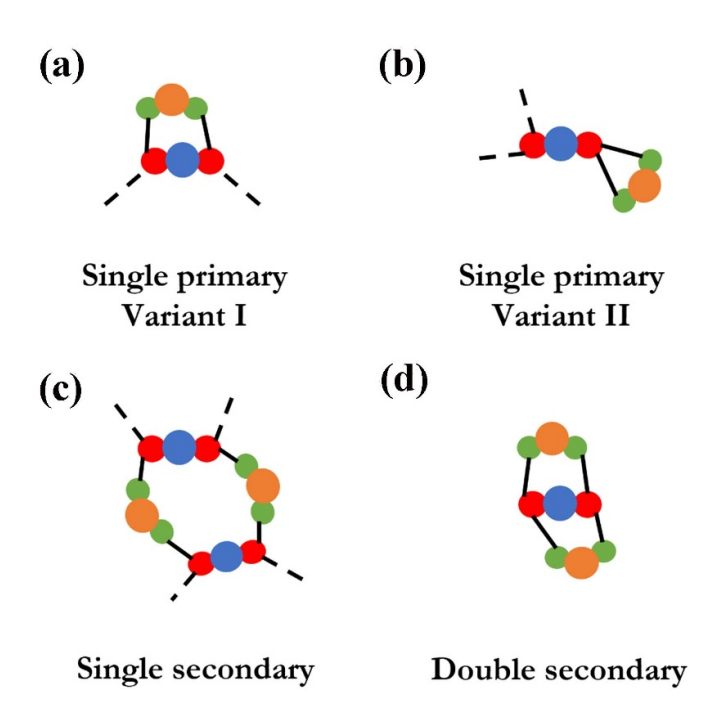


Figure 2. Schematics of primary and secondary loop types formed in the systems of interest in this work.

TSMPs. However, given that the shape memory properties are positively correlated with the total number of loops, it seems that non-defective loops (NDLs) have a positive effect on those properties. Thus, we split the total number of loops into two separate fingerprints: the number of DLs and the number of NDLs, which is the total number of loops subtracted by the number of DLs. In other words, NDLs are any loops that are not a DL. Given that we saw a positive correlation between both the shape recovery ratio as well as the recovery stress and the total number of loops, we expect the DLs to have adverse effects on the aforementioned properties, and we would also expect NDLs to have a positive effect on those properties.

DLs are identified as loops with a specific size: 6 for single primary-variant I loops (figure 2(a)), 4 for single primary-variant II (figure 2(b)), 12 for single secondary loops (figure 2(c)), and 8 for double secondary loops (figure 2(d)). It should be noted that double secondary loops count as three DLs: one secondary loop (with a size of 8 instead of 9, since the hardener's non-reactive atom (blue particle in figure 2(d))

Table 3. Pearson correlation coefficient and its corresponding p-value among the topological fingerprints: number of non-defective loops (NDLs) as well as the number of defective loops (DLs) and the mechanical and shape memory properties of the systems with random topologies: glassy elastic modulus ($E_{\rm g}$), rubbery elastic modulus ($E_{\rm r}$), shape recovery ratio ($R_{\rm r}$) and recovery stress ($\sigma_{\rm r}$). Results with statistical significance are highlighted in red.

	Numbe	r of NDLs	Number of DLs		
Property	\overline{r}	p	\overline{r}	p	
$\overline{E_{\mathrm{g}}}$	0.048	0.632	0.108	0.284	
$E_{ m g} \ E_{ m r}$	0.137	0.173	-0.125	0.214	
$R_{\rm r}$	0.201	0.044	-0.062	0.537	
$\sigma_{ m p}$	0.199	0.045	-0.170	0.091	
$\sigma_{\rm r}$	0.269	0.006	-0.197	0.0491	

does not participate in the formation of the larger loop) and two primary loops (single-variant I). Then, we calculated the correlation coefficient between the mechanical and shape memory properties and the two loop subsets (table 3).

Out of the ten possible correlations, five of them are statistically significant: positive correlations between the number of higher order loops and the programming stress, recovery stress, and the shape recovery ratio, and a negative correlation between the number of DLs and the programming stress and recovery stress. Thus, our assumption that the NDLs would have a positive effect on the properties of the TSMPs is proven to be valid. However, it should be mentioned that no statistically significant correlations were found between either the NDLs or DLs and the rubbery elastic modulus.

As evident from table 1, topology has a significant effect on the programming and recovery stress, while its effect on the rubbery elastic modulus is less pronounced. Both programming and recovery stress are measured at relatively higher levels of deformation (i.e. 50% compression), while the rubbery elastic modulus is measured at a lower level of deformation (i.e. overall, 3% compression/stretching). Therefore, it seems that topology impacts the properties of TSMPs at larger deformation. Furthermore, the fact that the number of DLs in our systems with random topologies is relatively small (only 18), coupled with the fact that the effect of topology is more substantial at higher deformation levels, can explain why these current fingerprints are still unable to capture the effect of topology on the rubbery elastic modulus. Moreover, in our

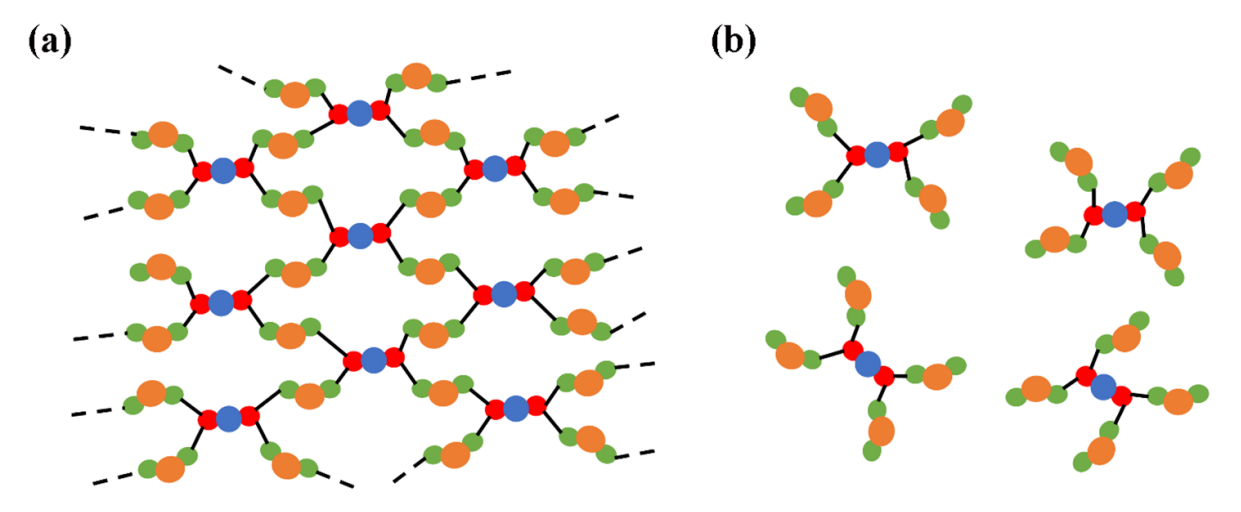


Figure 3. Schematic of (a) a complete, defect-free network and (b) tetra-distinctly-reacted (TDR) hardener molecules.

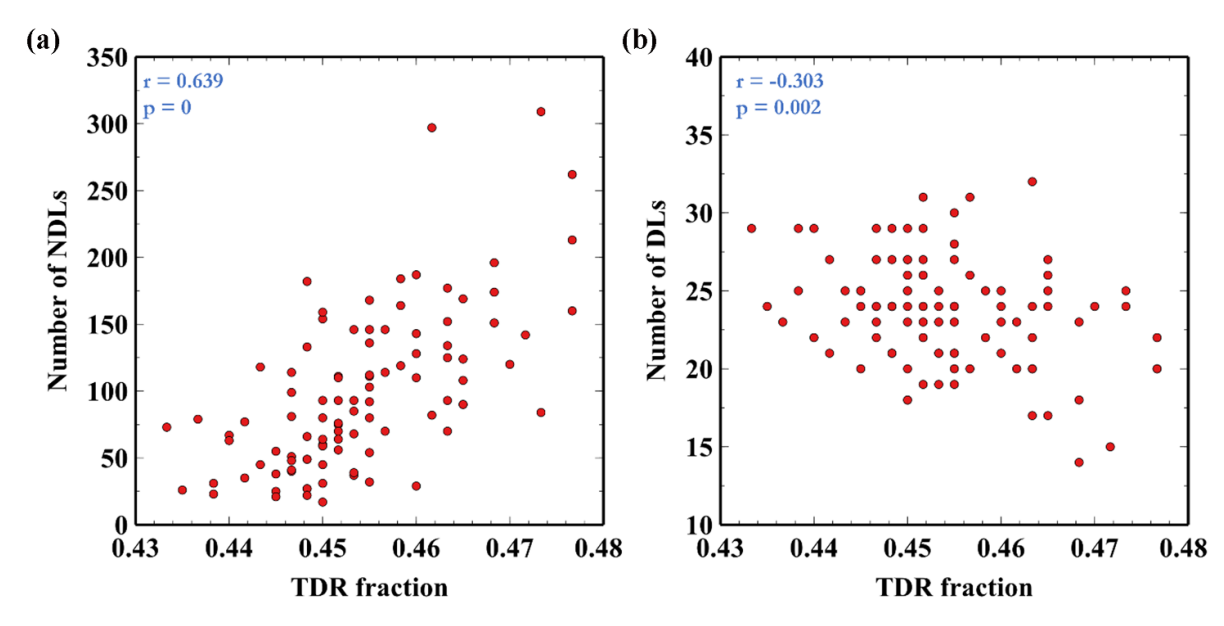


Figure 4. Plot of (a) the number of non-defective loops (NDLs) vs the fraction of tetra-distinctly-reacted (TDR) hardener molecules, and (b) the number of defective loops (DLs) vs. TDR fraction. The Pearson correlation coefficient (*r*) and its corresponding *p*-value (*p*) are presented in blue on the top-left corner of each plot.

analysis, NDLs consist of many loops of different orders. Characterizing the effects of loops of any individual order is a cumbersome task, given that not all systems are going to contain loops of every order. Thus, it is crucial to find a more generalized context to justify the observed effects of NDLs on the properties of TSMPs.

To do this, we considered a perfect network. DL are deviations from such a network. NDLs would then be associated with a more perfect network, the exact distribution of which depends on the distribution of DL. An increase in the number of NDLs would thus be expected to correlate with a more perfect network and thus correlate positively with both shape recovery ratio and recovery stress as found above.

The building blocks of a perfect network are defined as the hardener molecules that have bonded with as many distinct epoxy molecules as possible. In the case of the system of interest in this study, the number of unique epoxy molecules that can bond to a single hardener molecule is 4 (figure 3(b)). We name these specific hardener molecules TDR and introduce a new fingerprint: TDR fraction, which is the ratio of the number of TDR hardener molecules to the total number of hardener molecules present in the system. The correlation between the number of NDLs and DLs and the TDR fractions is presented in figure 4.

As evident from figure 4, the number of NDLs is positively correlated with the TDR fraction, and the number of DLs is negatively correlated with the TDR fraction. The correlations are relatively strong in both cases. Thus, it is elucidated that the number of NDLs and DLs are a measure of network perfection and how it is affected by the defects; the mechanical and shape memory properties of the system are indeed determined by the degree of network perfection and TDR fraction. To

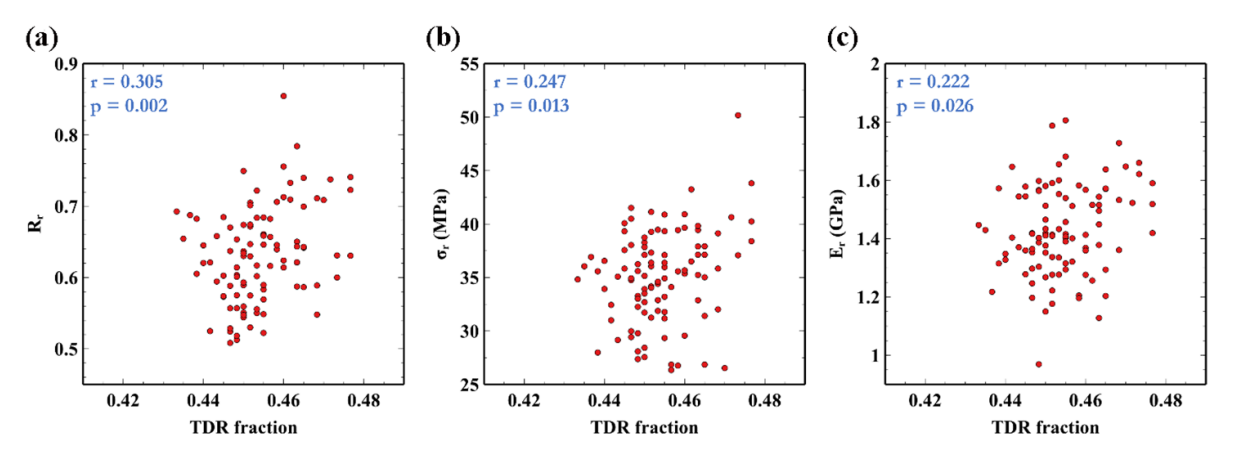


Figure 5. Plot of (a) shape recovery ratio (R_r) vs the fraction of tetra-distinctly-reacted (TDR) hardener molecules, (b) recovery stress (σ_r) vs. TDR fraction, and (c) rubbery elastic modulus (E_r) vs. TDR fraction. The Pearson correlation coefficient (r) and its corresponding p-value (p) are presented in blue on the top-left corner of each plot.

showcase this, the correlation between these properties and the TDR fraction is analyzed and those correlations with statistical significance are presented in figure 5.

It can be observed in figure 5 that not only the recovery stress and recovery ratio are positively correlated with the TDR fraction, but also the rubbery elastic modulus, as implied in the previous studies of the relationship between mechanical properties and cyclic topology in polymer networks. Interestingly, the correlation between the TDR fraction and the shape memory properties is stronger than that between the elastic rubbery modulus and the TDR fraction. It is also important to note that the correlation coefficient between the programming stress and the TDR fraction is 0.192, with a p-value of 0.055. We have strictly defined a statistically significant correlation as one with p < 0.5. However, that should not negate the strong effect of the topology on the programming stress as well.

Although our study focuses on only a single pair of hardener-epoxy, the fundamental result—that the enhancement of network perfection during the synthesis of TSMPs will increase desirable mechanical/shape memory properties of those materials—applies to this whole class of materials. Techniques such as semibatch monomer addition [69] could improve the network connectivity by increasing the TDR fraction in the system and ultimately result in the availability of more building blocks for the formation of a perfect network. Furthermore, modifying the number of functional groups on the hardener molecules could increase the probability of the formation of TDR hardener molecules. Finally, while increasing the overall crosslinking density of the system would enhance the network perfection, it would also increase the risk of defect formation in the system. Thus, attempts at increasing the overall crosslinking density should be complemented with methods that would increase the TDR fraction, during their synthesis. Implementing such techniques would lead to an overall decrease of defects in the system and thus, an improvement in shape memory properties, specifically the recovery stress. Moreover, such an approach can lead to an improvement in both recovery stress and shape recovery ratio, unlike other methods such as fiber/particulate reinforcement of TSMPs mentioned earlier.

5. Conclusions

Using molecular dynamics simulations and a CG model, the effect of cyclic topology on the mechanical and shape memory properties of a TSMP, DGEBA-DDM, was investigated. Hundred structures of the TSMP of interest with random topologies and 25 structures of the same system with a fixed topology were prepared. The statistical significance of the differences between the mean of mechanical properties (glassy and rubbery elastic modulus) as well as shape memory properties (recovery stress and shape recovery ratio) between the two groups of systems were evaluated by calculating the p-values. The differences in the rubbery elastic modulus, shape recovery ratio, and recovery stress between the two sets of systems were found to be statistically significant (p < 0.05) and resulted in variations greater than 33% and 25% in programming stress and recovery stress, respectively, while the variation in rubbery elastic modulus was only about 10%. This indicates that topology and network perfection are important indicators of shape memory performance. Moreover, the effect of topology seems to be more substantial at higher levels of deformation.

Inspired by the existing studies in the literature regarding the effect of loops and more specifically, DLs on the mechanical properties of the polymer networks, the correlations between the mechanical/shape memory properties of the systems and the number of loops as well as their average size and weight-averaged size, the number of DLs and the number of higher order loops were examined. Although it was found that the shape recovery ratio and recovery stress are positively correlated with the number of NDLs, and the recovery stress is negatively correlated with the number of DLs, no statistically significant correlations were found between any of the aforementioned topological fingerprints and the rubbery elastic modulus. Given that the number of higher order

loops and the number of DLs can be seen as measures of how a real network is closer to or deviates from a perfect network, it was then investigated whether the properties of the systems are correlated with any other features that are representative of the network completeness. Upon examining the correlation between the properties of the systems and the fraction of the hardener molecules that are reacted to four different epoxy molecules (TDR molecules, or TDRs), it was found that the rubbery elastic modulus, shape recovery ratio, and the recovery stress are all positively correlated with said fraction, and these correlations are stronger than those found with the number of DL or the number of NDLs. TDR is thus a proper measure of network perfection and a better descriptor for mechanical/shape memory properties, setting up a goal for new design and processing methods of thermoset shape memory epoxies.

The elucidation of the correlation between the mechanical as well as shape memory properties of TSMPs and the fraction of hardener molecules that have reacted with the maximum number of distinct epoxy molecules have very interesting implications in terms of the synthesis of TSMPs with improved properties, especially shape memory properties. Techniques such as semibatch monomer addition or conceptually similar methods can lead to an improvement in both shape recovery ratio and recovery stress, as opposed to other methods such as fabric/particulate reinforcement of the TSMPs, which sometimes lead to a loss of shape memory altogether. Moreover, topology alteration can also be explored to produce TSMPs with improved shape memory properties and not necessarily a higher stiffness, enabling even more control over the synthesis of these materials for more specialized applications. Exploring the impact of the number of functional sites per hardener molecule and the role of crosslinking density on the degree of network perfection will be the focus of future studies.

Data availability statement

The data that support the findings of this study are available upon reasonable request from the authors.

Acknowledgments

This work is funded by the US National Science Foundation under Grant No. OIA-1946231 and the Louisiana Board of Regents for the Louisiana Materials Design Alliance (LAMDA). All the simulations were conducted using the high-performance computing resources provided by the Louisiana Optical Network Infrastructure (LONI). Pouria Nourian would like to thank Behnam Taghavi Fard for discussions regarding the statistical analysis of the results.

ORCID iDs

Pouria Nourian https://orcid.org/0000-0001-5270-7639
Colin D Wick https://orcid.org/0000-0002-0261-0780
Guoqiang Li https://orcid.org/0000-0002-7004-6659
Andrew J Peters https://orcid.org/0000-0001-5031-2828

References

- [1] Flory P J 1944 Network structure and the elastic properties of vulcanized rubber *Chem. Rev.* **35** 51–75
- [2] Ratna D and Karger-Kocsis J 2008 Recent advances in shape memory polymers and composites: a review *J. Mater. Sci.* 43 254–69
- [3] Geise G M, Lee H-S, Miller D J, Freeman B D, McGrath J E and Paul D R 2010 Water purification by membranes: the role of polymer science J. Polym. Sci. B 48 1685–718
- [4] Shannon M, Bohn P, Elimelech M, Georgiadis J, Mariñas B and Mayes A 2008 Science and technology for water purification in the coming decades *Nanoscience and Technology* 452 301–10
- [5] Dawson R, Cooper A I and Adams D J 2012 Nanoporous organic polymer networks *Prog. Polym. Sci.* 37 530–63
- [6] Chen Q, Luo M, Hammershøj P, Zhou D, Han Y, Laursen B W, Yan C-G and Han B-H 2012 Microporous polycarbazole with high specific surface area for gas storage and separation J. Am. Chem. Soc. 134 6084–7
- [7] Yuan D, Lu W, Zhao D and Zhou H-C 2011 Highly stable porous polymer networks with exceptionally high gas-uptake capacities Adv. Mater. 23 3723–5
- [8] McKeown N B and Budd P M 2006 Polymers of intrinsic microporosity (PIMs): organic materials for membrane separations, heterogeneous catalysis and hydrogen storage *Chem. Soc. Rev.* 35 675–83
- [9] De Gennes P-G and Gennes P-G 1979 Scaling Concepts in Polymer Physics (Ithaca: Cornell University Press)
- [10] Flory P J 1953 Principles of Polymer Chemistry (Ithaca: Cornell University Press)
- [11] Mark J E and Erman B 2007 Rubberlike Elasticity: A Molecular Primer (Ithaca: Cambridge University Press)
- [12] Sun J-Y, Zhao X, Illeperuma W R K, Chaudhuri O, Oh K H, Mooney D J, Vlassak J J and Suo Z 2012 Highly stretchable and tough hydrogels *Nature* 489 133–6
- [13] He X, Aizenberg M, Kuksenok O, Zarzar L D, Shastri A, Balazs A C and Aizenberg J 2012 Synthetic homeostatic materials with chemo-mechano-chemical self-regulation *Nature* 487 214–8
- [14] Stuart M A C *et al* 2010 Emerging applications of stimuli-responsive polymer materials *Nat. Mater.* **9** 101–13
- [15] Lv S, Dudek D M, Cao Y, Balamurali M M, Gosline J and Li H 2010 Designed biomaterials to mimic the mechanical properties of muscles *Nature* 465 69–73
- [16] Wang Q, Mynar J L, Yoshida M, Lee E, Lee M, Okuro K, Kinbara K and Aida T 2010 High-water-content mouldable hydrogels by mixing clay and a dendritic molecular binder *Nature* 463 339–43
- [17] Discher D E, Mooney D J and Zandstra P W 2009 Growth factors, matrices, and forces combine and control stem cells *Science* 324 1673–7
- [18] Langer R and Tirrell D A 2004 Designing materials for biology and medicine Nature 428 487–92
- [19] Lutolf M P, Lauer-Fields J L, Schmoekel H G, Metters A T, Weber F E, Fields G B and Hubbell J A 2003 Synthetic matrix metalloproteinase-sensitive hydrogels for the conduction of tissue regeneration: engineering cell-invasion characteristics *Proc. Natl Acad. Sci.* 100 5413–8
- [20] Chen X, Dam M A, Ono K, Mal A, Shen H, Nutt S R, Sheran K and Wudl F 2002 A thermally re-mendable cross-linked polymeric material *Science* 295 1698–702
- [21] Lee K Y and Mooney D J 2001 Hydrogels for tissue engineering Chem. Rev. 101 1869–80
- [22] Guo Q 2017 Thermosets: Structure, Properties, and Applications (Cambridge: Woodhead Publishing)
- [23] Liu C, Qin H and Mather P T 2007 Review of progress in shape-memory polymers J. Mater. Chem. 17 1543–58

- [24] Liu Y, Du H, Liu L and Leng J 2014 Shape memory polymers and their composites in aerospace applications: a review Smart Mater. Struct. 23 023001
- [25] Lan X, Liu Y, Lv H, Wang X, Leng J and Du S 2009 Fiber reinforced shape-memory polymer composite and its application in a deployable hinge *Smart Mater. Struct*. 18 024002
- [26] Jin Yoo H, Chae Jung Y, Gopal Sahoo N and Whan Cho J 2006 Polyurethane-carbon nanotube nanocomposites prepared by in-situ polymerization with electroactive shape memory J. Macromol. Sci. B 45 441–51
- [27] Atli B, Gandhi F and Karst G 2009 Thermomechanical characterization of shape memory polymers J. Intell. Mater. Syst. Struct. 20 87–95
- [28] Maitland D J, Metzger M F, Schumann D, Lee A and Wilson T S 2002 Photothermal properties of shape memory polymer micro-actuators for treating stroke *Lasers Surg.* Med. 30 1–11
- [29] Li G and Xu T 2011 Thermomechanical characterization of shape memory polymer–based self-healing syntactic foam sealant for expansion joints *J. Transp. Eng.* 137 805–14
- [30] Santos L, Dahi Taleghani A and Li G 2018 Expandable proppants to moderate production drop in hydraulically fractured wells J. Nat. Gas Sci. Eng. 55 182–90
- [31] Mansour A, Dahi Taleghani A, Salehi S, Li G and Ezeakacha C 2019 Smart lost circulation materials for productive zones J. Pet. Explor. Prod. Technol. 9 281–96
- [32] Lendlein A and Langer R 2002 Biodegradable, elastic shape-memory polymers for potential biomedical applications *Science* **296** 1673–6
- [33] Tamai H, Igaki K, Kyo E, Kosuga K, Kawashima A, Matsui S, Komori H, Tsuji T, Motohara S and Uehata H 2000 Initial and 6-month results of biodegradable poly-l-lactic acid coronary stents in humans *Circulation* **102** 399–404
- [34] Ewert P, Riesenkampff E, Neuss M, Kretschmar O, Nagdyman N and Lange P E 2004 Novel growth stent for the permanent treatment of vessel stenosis in growing children: an experimental study *Catheter Cardiovasc*. *Interv.* 62 506–10
- [35] Vogt F *et al* 2004 Long-term assessment of a novel biodegradable paclitaxel-eluting coronary polylactide stent *Eur. Heart J.* **25** 1330–40
- [36] Lendlein A and Kelch S 2002 Shape-memory polymers Angew. Chem., Int. Ed. 41 2034–57
- [37] Wick C D, Peters A J and Li G 2021 Quantifying the contributions of energy storage in a thermoset shape memory polymer with high stress recovery: a molecular dynamics study *Polymer* 213 123319
- [38] Fan J and Li G 2018 High enthalpy storage thermoset network with giant stress and energy output in rubbery state *Nat. Commun.* 9 642
- [39] Ivens J, Urbanus M and De Smet C 2011 Shape recovery in a thermoset shape memory polymer and its fabric-reinforced composites *Express Polym. Lett.* **5** 254–61
- [40] Ni Q-Q, Zhang C-S, Fu Y, Dai G and Kimura T 2007 Shape memory effect and mechanical properties of carbon nanotube/shape memory polymer nanocomposites *Compos*. *Struct.* 81 176–84
- [41] Koerner H, Price G, Pearce N A, Alexander M and Vaia R A 2004 Remotely actuated polymer nanocomposites stress-recovery of carbon-nanotube-filled thermoplastic elastomers Nat. Mater. 3 115–20
- [42] Meng Q and Hu J 2009 A review of shape memory polymer composites and blends Composites A 40 1661–72
- [43] Gunes I S, Cao F and Jana S C 2008 Evaluation of nanoparticulate fillers for development of shape memory polyurethane nanocomposites *Polymer* 49 2223–34

- [44] Gall K *et al* 2002 Shape memory polymer nanocomposites *Acta Mater.* **50** 5115–26
- [45] Zhang C-S and Ni Q-Q 2007 Bending behavior of shape memory polymer based laminates *Compos. Struct.* 78 153–61
- [46] Gall K, Mikulas M, Munshi N A, Beavers F and Tupper M 2000 Carbon fiber reinforced shape memory polymer composites J. Intell. Mater. Syst. Struct. 11 877–86
- [47] Elliott J E, Nie J and Bowman C N 2003 The effect of primary cyclization on free radical polymerization kinetics: experimental characterization *Polymer* 44 327–32
- [48] Elliott J E and Bowman C N 2002 Effect of primary cyclization on free radical polymerization kinetics: modeling approach *Macromolecules* **35** 7125–31
- [49] Odian G 2004 Principles of Polymerization (New York: Wiley)
- [50] Syed I H, Stratmann P, Hempel G, Klüppel M and Saalwächter K 2016 Entanglements, defects, and inhomogeneities in nitrile butadiene rubbers: macroscopic versus microscopic properties *Macromolecules* 49 9004–16
- [51] Metters A and Hubbell J 2005 Network formation and degradation behavior of hydrogels formed by Michael-type addition reactions *Biomacromolecules* 6 290–301
- [52] Elliott J E, Macdonald M, Nie J and Bowman C N 2004 Structure and swelling of poly(acrylic acid) hydrogels: effect of pH, ionic strength, and dilution on the crosslinked polymer structure *Polymer* **45** 1503–10
- [53] Vorov O K, Livesay D R and Jacobs D J 2008 Conformational entropy of an ideal cross-linking polymer chain *Entropy* 10 285–308
- [54] Reneker D H, Kataphinan W, Theron A, Zussman E and Yarin A L 2002 Nanofiber garlands of polycaprolactone by electrospinning *Polymer* 43 6785–94
- [55] Beshah K, Mark J E and Ackerman J L 1986 Topology of poly(dimethylsiloxane) elastomeric networks studied by variable-temperature solid-state nuclear magnetic resonance *Macromolecules* 19 2194–6
- [56] Wang J, Lin T-S, Gu Y, Wang R, Olsen B D and Johnson J A 2018 Counting secondary loops is required for accurate prediction of end-linked polymer network elasticity ACS Macro Lett. 7 244–9
- [57] Wang R, Alexander-Katz A, Johnson J A and Olsen B D 2016 Universal cyclic topology in polymer networks *Phys. Rev. Lett.* 116 188302
- [58] Lin T-S, Wang R, Johnson J A and Olsen B D 2018 Topological structure of networks formed from symmetric four-arm precursors *Macromolecules* 51 1224–31
- [59] Akagi Y, Gong J P, Chung U-I and Sakai T 2013 Transition between phantom and affine network model observed in polymer gels with controlled network structure *Macromolecules* 46 1035–40
- [60] Zhong M, Wang R, Kawamoto K, Olsen B D and Johnson J A 2016 Quantifying the impact of molecular defects on polymer network elasticity *Science* 353 1264–8
- [61] Duan K, He Y, Li Y, Liu J, Zhang J, Hu Y, Lin R, Wang X, Deng W and Li L 2019 Machine-learning assisted coarse-grained model for epoxies over wide ranges of temperatures and cross-linking degrees *Mater. Des.* 183 108130
- [62] Dhamankar S and Webb M A 2021 Chemically specific coarse-graining of polymers: methods and prospects J. Polym. Sci. 59 2613–43
- [63] Brenner D W 1990 Empirical potential for hydrocarbons for use in simulating the chemical vapor deposition of diamond films *Phys. Rev.* B 42 9458
- [64] Plimpton S 1995 Fast parallel algorithms for short-range molecular dynamics *J. Comput. Phys.* 117 1–19
- [65] Nosé S 1984 A unified formulation of the constant temperature molecular dynamics methods J. Chem. Phys. 81 511–9

- [66] Shinoda W, Shiga M and Mikami M 2004 Rapid estimation of elastic constants by molecular dynamics simulation under constant stress *Phys. Rev.* B 69 134103
- [67] Abbott L and Colina C 2013 Polymatic: a generalized simulated polymerization algorithm for amorphous polymers *Theoretical Chemistry Accounts* **132** 1334
- [68] Shafe A, Wick C D, Peters A J, Liu X and Li G 2022 Effect of atomistic fingerprints on thermomechanical properties of
- epoxy-diamine thermoset shape memory polymers *Polymer* **242** 124577
- [69] Gu Y, Kawamoto K, Zhong M, Chen M, Hore M J A, Jordan A M, Korley L T J, Olsen B D and Johnson J A 2017 Semibatch monomer addition as a general method to tune and enhance the mechanics of polymer networks via loop-defect control *Proc. Natl Acad. Sci.* 114 4875